TIME EFFECTS IN THE STATIC TESTING OF CONCRETE TO DETERMINE FRACTURE ENERGY

by

Hoi Choong Siew

B.S., Kansas State University, 1984

A MASTER'S THESIS

submitted in partial fulfillment of the

requirements for the degree of

MASTER OF SCIENCE

Department of Civil Engineering

KANSAS STATE UNIVERSITY

Manhattan, Kansas

1986

Approved:

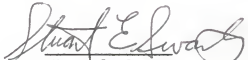

Major Professor

LD
2668
.T4
1986
S53
c.2

A11202 971363

TABLE OF CONTENTS

ACKNOWLEDGEMENTS

The author would like to express his sincere gratitude and appreciation to Dr. Stuart E. Swartz for his guidance and assistance in the course of graduate studies and production of this thesis. Thanks are also extended to Miss Sze Ting Yap, Mr. Ali Nikaeen, Mr. Randy Bernhardt and Mr. Russell Gillespie for their encouragement and assistance during testing.

Further acknowledgements are also extended to the author's parents, Mr. and Mrs. Siew Sow Wah, brother, Siew Kai Hong, sisters, Siew Mei Poh and Siew Mei Sin for their continuous moral support.

The work reported herein has been supported by the National Science Foundation on Grants CEE-8317136 and MSM-8317136. This support is gratefully acknowledged.

LIST OF TABLES

LIST OF FIGURES

NOTATION

a_o - Notch Length

b - Beam Width

CMOD - Crack Mouth Opening Displacement

E - Modulus of Elasticity

G_F - Fracture Energy, RILEM Method

$\overline{G_F}$ - Fracture Energy, Modified RILEM Method

K_I - Stress Intensity Factor for Opening Mode

L - Beam Length

LPD - Load Point Displacement

P_m - Maximum Load

P - Load

U - Energy Absorbed by the Beam up to Point of Instability

W_o - Energy Absorbed by the Beam up to Maximum Deflection

w - Beam Depth

δ_o - Vertical Displacement at Maximum Value

$\overline{\delta_o}$ - Vertical Displacement at Point of Instability

CHAPTER 1

INTRODUCTION

The effect of loading rate in the course of concrete testing has been under investigation for many years. It is generally agreed that loading rate has an effect on compression, flexure, and tensile tests. When the rate of application is increased, higher strength is reported in the three mentioned tests and lower strength when lower rates are used. However, in fracture mechanics, the effect of loading rate has not been studied extensively in the investigation of fracture energy (G_F).

To study the loading effect, i.e. the time effect of static testing of concrete in determining G_F, sixteen beams with a width of 3 in. (76 mm), a depth of 4 in. (102 mm), and a span of 15 in. (381 mm) were cast and tested in a three-point bending fashion. The beams were notched with a_o/w of 0.3, 0.5, and 0.7. Two loading modes were used in the testing, namely, load control and strain control. A detailed description of the experimental program is found in Chapter 3.

The results obtained showed that the values of G_F were relatively consistent for the loading rate used in the experiment. Time to peak load for the beams ranged from 34 to 225 seconds. However, to obtain consistent and relevant results, a systematic computation technique for time to reach peak load is desired, where it will depend on initial notch length, size, and peak load of the beam. G_F calculated using the RILEM Method showed strain control should be used in the testing because G_F from load control gave consistently higher results when compared to

values from strain control. However, when the Modified RILEM Method was used, the mode of testing control made no difference, i.e., values of $\overline{G_F}$ from both controls were fairly consistent. These results, summary and conclusions are presented in Chapter 4 and Chapter 5.

CHAPTER 2

REVIEW OF LITERATURE

2.1 Standard Method of Concrete Testing

The structural properties of concrete are, among other things, a function of time and ambient humidity. For this reason, the conditions of its testing are extremely important to obtain relevant data. The most common test on concrete is probably its strength test, either in compression or tension. The conditions that will affect the testing results range from stiffness of machine, loading rate, condition of the concrete specimen, to human's limitation. However, this report will examine mainly the effect of the rate of loading in concrete testing.

In this section, different standard strength testing methods of concrete will be briefly reviewed. Strength testing in concrete is mainly divided into two categories: 1) destructive, and 2) non-destructive tests. Since this report deals mainly with loading effect, non-destructive tests will not be discussed. The standard destructive tests that will be discussed are the compression test, flexure test, and splitting test. Another standard destructive test where loading from the testing machine is not required, is the pullout test. Non-destructive tests that are commonly used are the rebound hammer test, penetration test, ultra pulse, and velocity test.

In compression testing, three different methods are available. They are the cylinder test, cube test, and prism test. In the United States, cylinder testing is most commonly used, while cube testing is popular in Europe. However, there is a tendency now in research where

cylinder testing is preferred over cube testing.

In the cylinder test, the standard concrete specimen is 6 inches (152 mm) in diameter, 12 inches (305 mm) long and should be cast in a mould that is made of steel, cardboard, or plastic. During casting, it is necessary to finish the top surface for smoothness for the purpose of testing. A capping material such as sulphur is normally used to ensure smoothness at the ends of the cylinder. Details of the casting procedure are prescribed in ASTM Standard C192-76 (3). The test method should conform to ASTM Standard C39-81 (1). The standard requires that the testing machine should be able to provide sufficient capacity and be capable of operating at a rate of 0.05 in. (1.3 mm)/min when the machine is running idle, if it is a screw-typed machine. In a hydraulically operated machine, load rate is required to be constant, within the range of 20 to 50 psi (0.14 to 0.34 MPa)/sec. During the first half of the load test, application of a higher load rate is permitted. No adjustment can be made on the machine as soon as the specimen begins to fail.

For the cube specimen, the dimension that is normally used is around 6 inches (150 mm), and should conform to a cubical shape. The specimen is suggested to be cast in steel or cast iron moulds. The British method of placing concrete into the cubical mould is fully explained in its code; BS 1881:Part3:1970 (6). Like its cylindrical counterpart, the top surface of the cube must be smooth for good testing results. Part four of the same code prescribes that applied load during testing should be at a constant rate of stress of 2220 psi/min (0.25 MPa/sec). In the prism test, the specimen is cast and tested almost the

same way as in the cube test.

In the flexure test, which is a measure of the tensile property of concrete; the concrete beam is tested by third-point loading. Flexure testing is, in fact, one of the two standard tensile tests, while the direct tension test is often disregarded because of difficulty in testing. From the flexure test, the maximum tensile stress at the bottom fibre of the beam can be estimated. This is known as the modulus of rupture. The British code specifies the specimen to have a size of 150 by 150 by 750 mm (6 by 6 by 30 in.) On the other hand, the ASTM Standard requires the test specimen span to be three times longer than its depth. In the United States, the standard method for flexure testing can be found in ASTM Standard C78-75 (2). The specification prescribes that the load should be applied continuously with a rate between 125 and 175 psi/min (14 and 206 Pa/sec) in the increment of the extreme fiber stress until rupture occurs. Like cylinder testing, higher rates can be used up to half of the specimen's failure load. The British code specifies similar rates for its standard flexure test.

Another standard method of measuring tensile strength is the splitting test. This test is done on concrete cylinders, similar to the one used in the compression test. The test is carried out by placing the concrete cylinder with its longitudinal axis's horizontal section between the platens of a testing machine. The load is then increased until failure in the form of splitting along the vertical diameter occurs. ASTM Standard C496-71 (4) requires the load to be applied continuously without shock at constant rates of 100-200 psi (689 - 1380 kPa)/min. This test is also covered by the British code, BS 1881:Part 4:1970 (6). The advantage of the splitting test is that a similar type

of specimen from this test can also be used in the compression test.

2.2 Effect of Loading Rate in Compression, Flexure, and Tensile Testing of Concrete

Over the years, many researchers have investigated the problem of the influence of rate application of load on concrete strength. Most of the investigations were done using cylinders, unreinforced beams, and reinforced beams.

Generally, it is understood that the rate of application has an effect on the apparent strength of concrete. The lower the rate of the stress increase the lower the strength that is obtained. A number of investigators have discovered that when the rate of application is increased in the compression test, apparent strength in concrete will increase. It is thought that this is due to the increase in strain with time because of creep. Also when limiting strain is reached, failure would occur independently of the value of the stress applied.

Price (23) discovered that when concrete was loaded at the rate of 30 psi (207 kPa)/second, the concrete can withstand stress up to only 70% of the ultimate strength. However, McHenry and Shideler (19) found that when concrete specimens were loaded in compression over 30 to 340 minutes, failure at 84 to 88 percent of the ultimate strength was obtained when the similar load rate was used. McHenry and Shideler (19) also found that when the rate of application increased from 0.1 psi (0.70 kPa)/sec to 10^7 psi (6.89×10^7 kPa)/sec, apparent strength was doubled. Figure 2.1 shows strength of concrete in compression at various loading rates.

Newman (21) in another compression test investigation, discovered

that when loading rate was about 10 x 10^6 kPa/sec (1.4 x 10^6 psi/sec) the cylinder strength was increased by about 50%, while cube strength increased by 25%, when compared to a standard loading rate of 200 kPa/sec (29 psi/sec). It was indicated that the 25% increase for the cube was probably due to the difference in relative extension of the loading-machine platen zone of influence, over the specimen's height. Rüsch (26) also found that when loading rate was below the standard value, strengths dropped down to 75-80% of the reference strength value.

In similar research, Dilger, et al. (8) tested plain and reinforced concrete prisms in compression, where they were subjected to strain rates of 0.2 in./in.-sec and 3.3x10^{-5} in./in.-sec. Plain concrete strength increased by about 35% when the strain rate was 0.2 in./in.-sec, when compared to the values obtained from a standard loading rate.

Similar to compression tests, flexure tests are also known to be dependent on the effect of loading rate. Wright (35) discovered that when the rate of stress in the extreme fiber was increased from 0.15 MPa (0.02 ksi)/min to 7.8 MPa (1.13 ksi)/min, the modulus of rupture that was obtained was increased by about 15%. Galloway and Raithby (9) in a similar research confirmed Wright's finding. These two tests reported a linear straight line relation exists between the modulus of rupture and the logarithm of the rate of application of stress. McNeely and Lash (20) found the same results in another similar research and Figure 2.2 illustrates the relationship.

In the tensile test, the rate of increase in loading, has shown effects on the tensile strain capacity. Komlos (17) experimented with two different loading rates, namely 711 psi (4.90 MPa)/min and 213 psi

(1.47 MPa)/min in uniaxial tension. The lower rate results exhibited a higher relative tensile strain. Lin and McDonald (18) found that when the tensile specimen was loaded at a slow loading rate of 25 psi (0.17 MPa)/week, the strain capacity was 1.1 to 2.1 greater than when the rate of loading was 0.68 psi (4.70 kPa)/sec.

2.3 Effect of Loading Rate in Linear Elastic Fracture Mechanics (LEFM) Testing of Concrete

Various experimental programs have been carried out to investigate the validity of the application of LEFM for concrete. Numerous fracture parameters are suggested in these experimental programs. Because of the relative infancy stage of the application of LEFM for concrete, experimental techniques have yet to be standardized. However, numerous experimental programs have been proposed, most notably that by the group RILEM TC50-FMC, Fracture Mechanics of Concrete (24).

Before continuing, it is necessary to elaborate more about the concept of application of LEFM for concrete. The acceptability of LEFM for concrete has thus far been questioned by the research community. This is due to the inconsistency of results from experimental methods obtained by many researchers when LEFM is applied to the problem of crack propagation and fracture in concrete.

For LEFM to be valid for concrete, for example for Type I displacement, certain conditions must hold true. Fracture toughness (K_{IC}) has to exist where it is associated with the onset or continuation of unstable crack growth. K_{IC} also has to be independent of crack length beyond some length and of specimen size. Another parameter, the energy release rate associated with unstable crack growth (G_{IC}) has to

be equivalent to K_{IC}. The J-Integral concept should produce results which are identical to G_{IC}. Also, a "process zone" must be small-if it exists-when compared to specimen dimensions and crack length.

Most of the fracture parameters mentioned are developed from bending specimens, especially three-point bending. From three-point bending specimens, values that are usually recorded in testing are crack mouth opening displacement (CMOD) and load point displacement (LPD) with their respective load readings. The specimen is often loaded to failure with constant application rate. The stress intensity values at peak load using initial crack lengths (K_I) and fracture toughness values using extended crack lengths (K_{IC}) can be computed using the formula developed by Go and Swartz (10). In this formula, a least squares method is used and it is a function of specimen size, pre-cracked depth, and maximum load. The energy release rate can then be obtained from the calculated K_I. The energy release rate can also be obtained directly from the area under the load versus LPD curve. When it is computed this way, it is known as fracture energy (G_F).

Up to now, investigators in this field have obtained results that were often size-dependent and gave considerable scatter such as reported by Hillerborg (13,14,15). The reasons for these inconsistencies according to Swartz, et al. (10,11,29,33), were due to not considering initially-cracked beams and ignoring crack growth. In all, investigators in this field have yet to agree on the experimental and theoretical approach. It is the purpose of this section to review investigations that have taken loading rate effect into account in their research of LEFM for concrete.

In the course of fracture mechanics testing, the progress of the

crack is usually monitored closely. The stages of growth can be summarized in five stages, as shown by Swamy (27). They are : 1) initiation of crack, 2) slow stable crack growth, 3) crack arrest, 4) critical crack condition, and 5) unstable crack propagation. The mode of fracture can normally be seen in three modes. They are: 1) catastrophic fracture, 2) semi-stable fracture, and 3) stable fracture as discussed by Ziegeldorf (36). These three modes of fracture are shown in Figure 2.3, with their typical load-deflection diagrams.

To investigate the effect of crack growth rate on fracture toughness (K_{IC}), Brown and Pomeroy (7) used double-cantilever-beam specimens with crack growth rates of about 0, 5, 35, and 1100 mm/min. The experiment showed that the toughness increased smoothly with crack growth. The toughness at the fastest speed was about 25% larger then at the slowest. Higgins and Bailey (12) found similar results with three-point bending specimens.

For many researchers, loading modes are normally carried out by deformation control or load control. Researchers recognised the advantages of these two loading modes. Load control is where the speed of the testing machine's piston reaches a certain load in a specified time where it is usually at a constant rate. Hydraulically-controlled machines and the MTS machine are normally run using load control. The MTS machine is a very versatile testing machine because it also can be run under deformation control. Two different deformation controls can be used with the MTS machine, namely strain control and stroke control. In stroke control, the deformation of the piston is the source of loading rate while strain control can be obtained by using a strain gage

device to measure the deformation of either the test specimen or the machine's piston. Another machine that can be operated under deformation control is a screw-type machine.

Swartz was the first to capitalize on the advantages of both strain and load control (28). Using an electro-hydrodynamic testing system (MTS), these two modes of control were carried out on concrete beams. With strain control, cracks can be grown to any reasonable depth and thus make precracking possible. This is often necessary before loading the specimens to failure where load control is used. A series of tests were carried out by Swartz, et al. (29,30,32,33,34) using the above two modes of control. From these tests, critical fracture toughness (K_I) values obtained from statically precracked versus fatigue precracking were virtually identical (30). It was also found that K_I values and failure loads for cracked beams were much higher than notched beams and it was concluded that notched beams were not suitable test specimens for determining fracture toughness (29). To obtain consistent results for the fracture parameters, it was considered necessary to determine the crack front by using a dye technique and consider slow crack growth to the point of instability (11,32,33). Along with the consistency in energy results (11,31,32,34), Swartz (31) therefore concluded LEFM is indeed suitable for concrete.

Hilsdorf and Brameshuber (16) also utilized these specific loading controls in their fracture mechanics research. Strain control at a rate of 0.1 mm/min of cross head speed was used for small beams. The same rate was also used for constant deflection of medium and large beams during the testings. It was found that the fracture energy (G_F)-values obtained from the experiments where rate of deflection was kept constant

were identical to G_F-values from specimens subjected to a sequence of loading and unloading.

According to Petersson (22), it was necessary to use displacement control if a stable fracture was desired in calculating G_F. If load control was used instead, unstable fracture would occur after maximum load is reached due to dynamic effects. To obtain stable fracture, it is also necessary for the crack to be able to consume exactly the amount of energy that is released from the beam and the testing machine during deformation. A problem that might arise according to Petersson is the long "tail" on the load-deflection curve in evaluating G_F. Theoretically, this tail is infinitely long and therefore finding the area under the curve would be a problem when determining G_F. Petersson also claimed that a small fault in the balance of the system if a long beam is used could create substancial error due to the long tail. To correct these problems, Petersson suggested to stop the test at a certain moment during testing to correspond to the uncorrected beam weight. However, he did not elaborate on the definition of "certain moment" and how it will give better test results. The testing time from start to maximum load was 30 seconds. However, Petersson did not explain why this speed was chosen.

Bazant (5), in his proposal to RILEM specified that the specimens should be loaded at a constant or almost constant displacement rate. He also stated that the loading rates should reach the maximum load within one to ten minutes while other loading rates may be used for special purposes. According to Bazant, the displacement rate should be optimally chosen in such a way that the theoretical velocity of the

crack tip is the same at maximum load for all specimens. Like Petersson above, Bazant did not explain why the specified displacement rates were chosen and how other loading rates can be correctly used in special purposes.

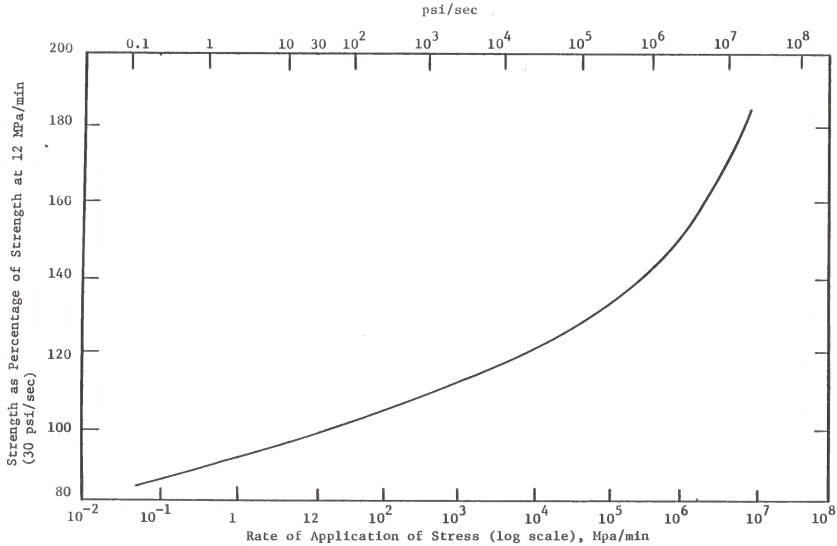

Figure 2.1 Influence of the Rate of Application of Load on the Compressive Strength of Concrete (19)

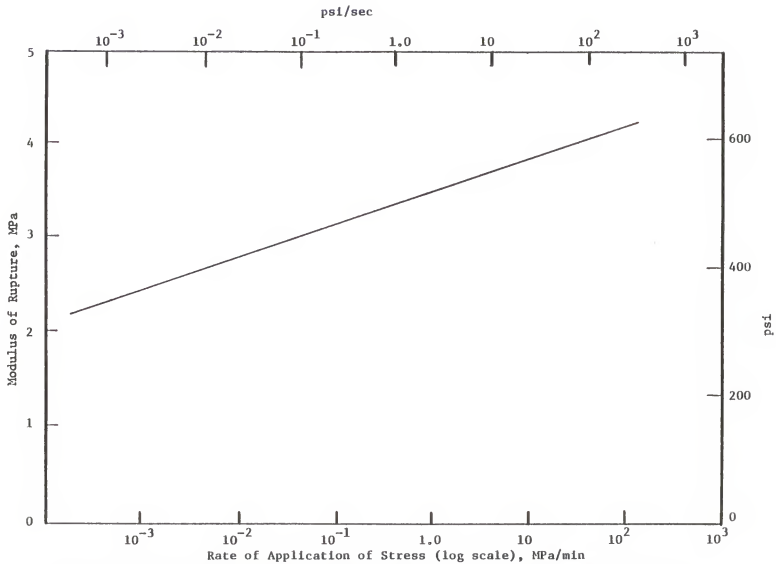

Figure 2.2 Influence of the Rate of Application of Load on the Modulus of Rupture of Concrete (20)

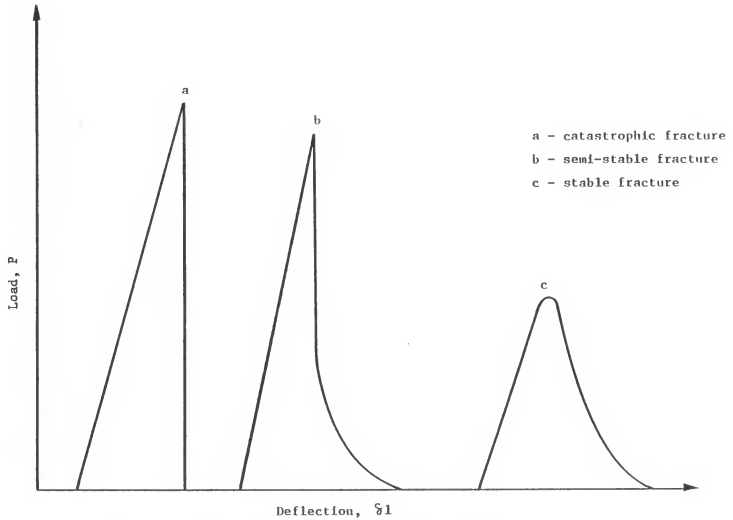

Figure 2.3 Typical load-deflection diagrams of hardened cement paste (36)

CHAPTER 3

EXPERIMENTAL PROGRAM

3.1 Test Specimens

The beams that were used in this experiment consist of one size only, with the following dimensions:

s = 15 in. (381 mm)
w = 4 in. (102 mm)
b = 3 in. (76 mm)

A sketch of the typical beam can be seen in Figure 3.1. One mix design was used for all the beams as shown in Table 3.1. A total of sixteen beams were cast from one batch of concrete mix while six 3 in. x 6 in. (76 mm x 152 mm) cylinders were cast for compressive strength testing. Two groups of three cylinders each were tested in two different machines, namely the Emery-Tatnall machine (300 kip capacity) and Southwark-Emery machine (70 kip capacity). In each group, load deformations were obtained using a compressometer.

Of the sixteen beams cast, all were initially notched with a concrete saw. Six beams had a_o/w of 0.3, six beams had a_o/w ratio of 0.5, and four beams had a_o/w of a ratio of 0.7.

The nominal compressive strength from cylinders tested with the Emery-Tatnall machine was 6170 psi (42.51 MPa) and a Modulus of Elasticity of 5.02×10^6 psi (34.59×10^3 MPa) was obtained while cylinders tested with the Southwark-Emery machine had a compressive strength of 5300 psi (36.50 MPa) and a Modulus of Elasticity of 3.84×10^6 psi (26.46×10^3 MPa). The reason for the difference between the two machine's values was because of error in the Southwark-Emery machine due to lack of calibration and also due to much lower stiffness.

Therefore, only values from the Emery-Tatnall will be refered to. Figure 3.2 shows stress versus strain values from the cylinder tested in the Emery-Tatnall machine.

3.2 Testing Machine and Setup

An electro-hydraulic materials testing machine (MTS) was used in the entire testing program. The load application mode was in three-point bending as shown schematically in Figure 3.1. Traces of both load versus crack mouth opening displacement (CMOD) and load versus load point displacement (LPD) were obtained simultaneously during the loading of each beam using displacement transducers (MTS 632.05 B-60) with a sensitivity of + 0.002 in. (+ .0508 mm) per 10 volt, full scale output.

As mentioned in the literature review, the MTS can apply load in three different modes, i.e., load, strain, and stroke controls. In this experiment, only load and strain controls were utilized. In load control, span controls the amount of load as the primary feedback with a constant load rate. In strain control, the span controls the displacement of the CMOD transducer as the primary feedback. Strain control enables the specimens to crack in a controllable manner.

It is important to have appropriate scale settings on the plotter to obtain good traces. A summary of X and Y-axis scale settings is shown in the next page where the X-axis corresponds to displacement. The plotters used for both traces were MTS 431.13A - 02 (Type 200 Control Mode).

Span and the frequency controls on the MTS dictate the rate at which load is applied to the beams.

X-axis Metric Setting

Ranges using Calib. setting:

0.5% per cm = 0.05 V/cm
1.0% per cm = 0.10 V/cm
2.5% per cm = 0.25 V/cm
5.0% per cm = 0.50 V/cm
10.0% per cm = 1.00 V/cm

CMOD - Range 2 $\pm$ 1 X 10^{-2} in./10V = $\pm$ 1 X 10^{-3} in./V

0.5% : 1 cm = 5.0 X 10^{-5} in.
1.0% : 1 cm = 1.0 X 10^{-4} in.
2.5% : 1 cm = 2.5 X 10^{-4} in.
5.0% : 1 cm = 5.0 X 10^{-4} in.

CMOD - Range 1 $\pm$ 2 X 10^{-2} in./10V = $\pm$ 2 X 10^{-3} in./V

0.5% : 1 cm = 1 X 10^{-4} in.
1.0% : 1 cm = 2 X 10^{-4} in.
2.5% : 1 cm = 5 X 10^{-4} in.
5.0% : 1 cm = 1 X 10^{-3} in.

LPD - Range 2 $\pm$ 9.72 X 10^{-4} in./V

0.5% : 1 cm = 4.86 X 10^{-5} in.
1.0% : 1 cm = 9.72 X 10^{-5} in.
2.5% : 1 cm = 2.43 X 10^{-4} in.
5.0% : 1 cm = 4.86 X 10^{-4} in.

LPD - Range 1 $\pm$ 19.08 X 10^{-4} in./V

0.5% : 1 cm = 9.54 X 10^{-5} in.
1.0% : 1 cm = 19.08 X 10^{-5} in.
2.5% : 1 cm = 4.77 X 10^{-4} in.
5.0% : 1 cm = 9.54 X 10^{-4} in.

Y-axis Metric Setting

Ranges using Calib. setting:

0.5% per cm = 0.05 V/cm
1.0% per cm = 0.10 V/cm
2.5% per cm = 0.25 V/cm
5.0% per cm = 0.50 V/cm
10.0% per cm = 1.00 V/cm

CMOD and LPD - All Ranges 1.0 V = 1000 lbs.
Using load cell with X 10

0.5% : 1 cm = 50 lb.
1.0% : 1 cm = 100 lb.
2.5% : 1 cm = 250 lb.
5.0% : 1 cm = 500 lb.

A typical setting used in the testing is shown below:

Model 410.21 Panel

Functions:	Upward ramp function
Frequency range:	0.1/1.1
Frequency:	1.0

406 Controller

Cal Factor:	4.21
Excitation:	4.41
Gain:	8
Rate:	4.6
ΔP:	0
FDBK Select:	XDCR2 = load control EXT = strain control

3.3 Testing Procedure

All beams were tested in a similar fashion with the only exception being in the type of loading control. Half of each of the three different groups of beams with a_o/w of 0.3,0.5, and 0.7 were separated. One half of the group was tested in strain control and the other half in load control. The time used to reach peak load is recorded for each beam in Table 4.1 and Table 4.2 and may also be seen on the beam traces presented in Appendix II.

Before the beam was placed on the machine in a three-point-bending loading fashion, it had the yoke (Figure 3.3) and CMOD transducer mounted on it (25). During the testing, it was found that it was absolutely necessary to have the edges of the beam that are placed on the supporting roller be smooth. This was because irregular edges would cause slippage which showed up on the load versus LPD trace during the process of loading.

After the beam was placed on the machine, the loading head was

raised to where it barely touched the beam, with no load being applied. Then, the LPD transducer was attached to the system as shown in Figure 3.4. The beam was then loaded to failure with its appropriate mode of loading. With load control, the beam was always broken into two pieces after failure. In strain control however, that did not happen. The controlled-cracking in the beam ran out of the transducer range during the the final stage of the loading. Traces of load versus CMOD and load versus LPD were obtained during the entire loading process. This procedure was repeated for all sixteen beams. The load versus load-point-displacement (LPD) traces appear in Appendix II.

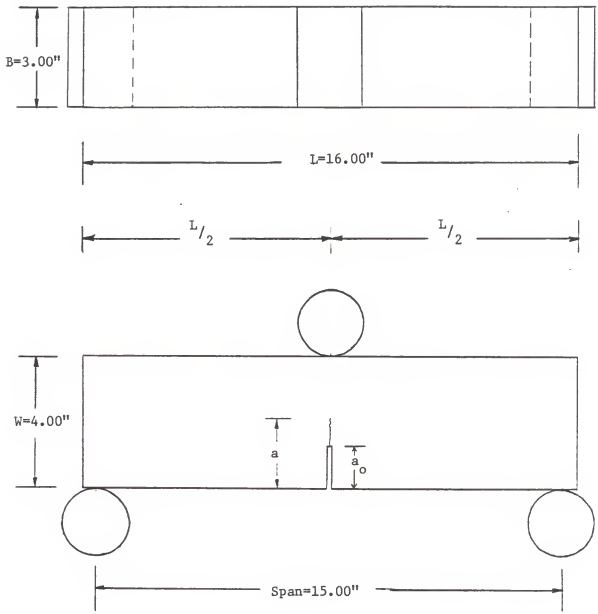

1.0 in. = 25.4 mm

Figure 3.1 Three Point Bending Configuration (25)

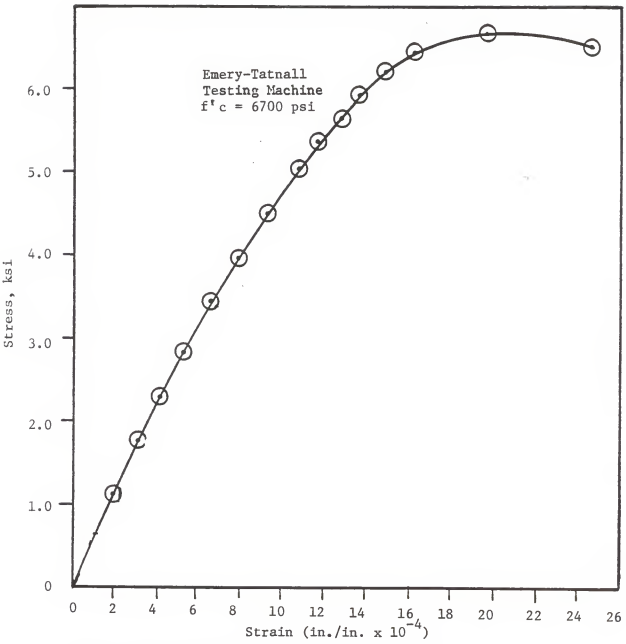

Figure 3.2 Cylinder Compressive Stress-Strain

1 ksi = 6.89 MPa

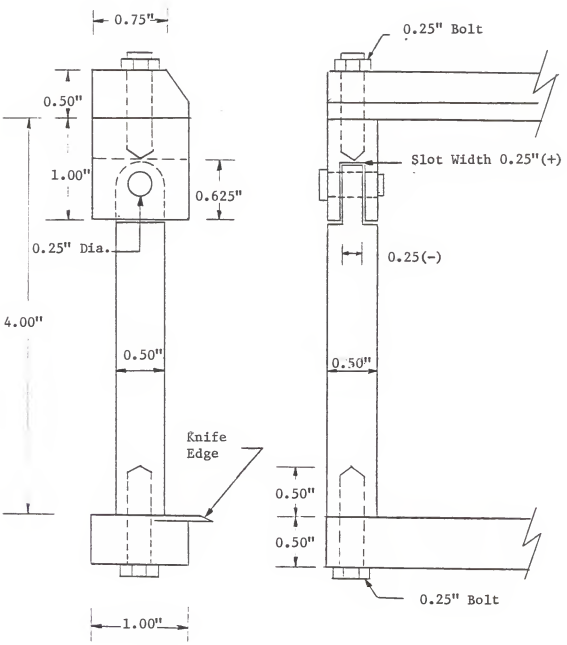

1.0 in. = 25.4 mm

Figure 3.3 CMOD Transducer Yokes (25)

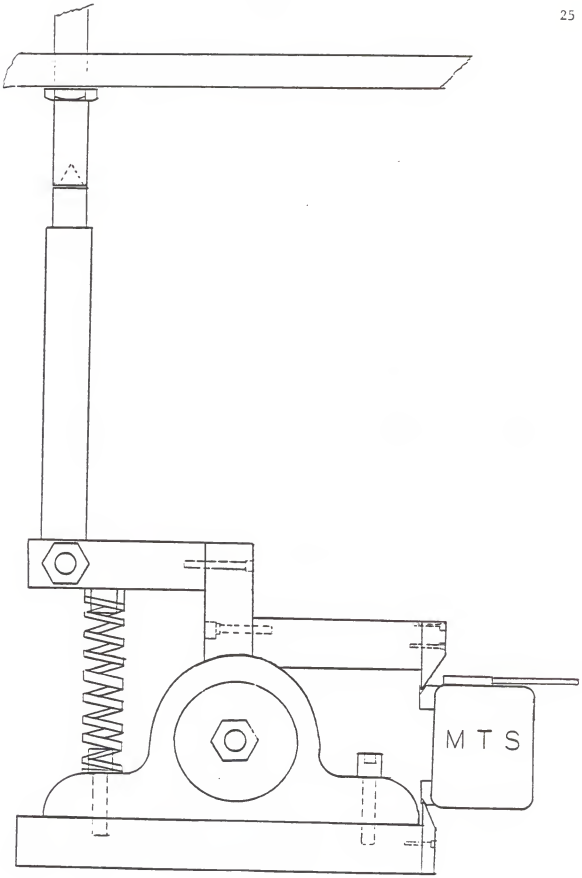

Figure 3.4 LPD Transducer Set Up (10)

Table 3.1 Mix Design

Water/Cement	0.5	
Cement Type	I	
S.G. Sand	2.65	
S.G. Aggregrate	2.56	
S.G. Cement	3.15	
% Sand by weight	32.64% (47.94 lb/ft^3)	0.2899 ft^3
% Aggregrate by weight	47.42% (69.65 lb/ft^3)	0.4360 ft^3
% Cement by weight	13.22% (19.42 lb/ft^3)	0.0988 ft^3
% Water by weight	6.03% (8.85 lb/ft^3)	0.1419 ft^3
% Super plasticizer by weight (S.G.=2)	0.70% (392ml) (1.03 lb/ft^3)	0.0137 ft^3
Unit weight of concrete	146.89 pcf	
Curing time	118 days	
Compressive strength (average)	6170 psi	
Slump	4.00 in.	
Vol. air (est)	0.02 ft^3	
Sand Fineness Modulus	2.91	
Maximimum aggregrate size	0.75 in.	

CHAPTER 4

EXPERIMENTAL RESULTS

4.1 Evaluation of Fracture Energy (G_F)

The sixteen beams were tested and traces of load versus LPD and load versus CMOD were obtained as previously described. For the purpose of this report, only load versus LPD plots will be used. Drawings of these are presented in Appendix II. Fracture energy release rate, which is defined as the amount of energy necessary to create one unit of area of a crack, is obtained from the area under the curve of load versus LPD. The question of whether the entire area, or just the area from the beginning of the load to the point of instability, should be considered in determining G_F arises among some researchers. Two different methods of evaluating G_F are therefore available, namely the RILEM Method (24) and the Modified RILEM Method proposed in Reference 34. The former method considers the entire area under the curve, while the latter method only considers the area from the beginning of applied load to the point of instability.

(a) RILEM Method

As previously stated, this method considers the entire energy consumed by the beams, i.e., the entire area in the load versus LPD curve in determining G_F. The reason the entire area is used is because of difficulty in defining the position of the tip of a propagating crack. Therefore, it is proposed that all the energy absorbed by the beam should be considered (24).

The formula for the RILEM Method is shown below (24):

$$G_F = \frac{W_o + mg\delta_o}{B(W - a_o)} \qquad 4.1$$

W_o = area under the entire curve, in.-lb (Nm)
mg = weight of the beam , lb (kN)
δ_o = maximum value of vertical displacement, in. (m)
B = width of beam, in. (m)
W = depth of beam, in. (m)
a_o = initial crack length, in. (m)

When the beam is loaded downward, mg is positive while mg is negative when the beam is loaded upward. Figure 4.1 shows a typical load versus LPD curve with W_o and δ_o clearly marked.

Values of energy released (W_o) in this method of calculation, i.e., the area under the entire curve, are listed in Table. 4.1. The average of values of W_o for strain-controlled beams were 2.60 lb-in. (0.295 N-m), 1.09 lb-in. (0.123 N-m), and 0.584 lb-in. (0.0660 N-m) for average a_o/w of 0.3, 0.5, and 0.7 respectively. The average values of W_o of load-controlled beams were 2.91 lb-in. (0.329 N-m), 1.86 lb-in. (0.210 N-m), and 0.661 lb-in. (0.0746 N-m) for average values of a_o/w of 0.3, 0.5, and 0.7 respectively.

The fracture energy per unit area using the Rilem Method was calculated for all sixteen beams. These values are listed in Table 4.1. The beam designations, "S" and "L" denote the loading mode, strain and load control respectively.

Average values for G_F for strain-controlled beams were 0.320 lb-in./in.^{2} (56.1 N-m/m^2), 0.205 lb-in./in.^{2} (35.9 N-m/m^2), and 0.195 lb-in./in^2 (34.2 N-m/m^2) for average a_o/w of 0.3, 0.5, and 0.7 respectively. Average values for G_F for load-controlled beams were

0.377 lb-in./in.^{2} (66.0 N-m/m^2), 0.351 lb-in./in^2 (61.6 N-m/m^2), and 0.216 lb-in./in.^{2} (37.8 N-m/m^2) for average a_o/w ratio of 0.3,0.5, and 0.7 respectively. Other average values are given in Table 4.3. Figure 4.3 shows a plot of G_F versus a_o/w using values from the RILEM Method.

(b) Modified RILEM Method

This method only considers energy absorbed by the beam to the point of instability as previously described. The point of instability is defined as the point on the load versus LPD curve where the load begins to drop off. The reason behind the development of this method is because it is felt that the rapid cracking after the point of instability makes it difficult to evaluate the energy data since the area available to resist cracking changes rapidly. The formula of this method is shown below:

$$\overline{G_F} = \frac{U + mg\overline{\delta_o}}{B(W-a_o)} \qquad 4.2$$

U = area under the curve up to point of instability, in.-lb (Nm)
mg = weight of the beam, lb (kN)
$\overline{\delta_o}$ = vertical displacement at point of instability, in. (m)
W = depth of the beam, in. (m)
a_o = initial crack length, in. (m)

Figure 4.2 shows a typical load versus LPD curve with U and δ_o clearly marked.

Values of energy (U) consumed by the beam as calculated by Modified RILEM Method are listed in Table 4.2. The average values of U of strain-controlled beams were 1.66 lb-in. (0.188 N-m), 0.593 lb-in. (0.0670 N-m), and 0.190 lb-in. (0.0215 N-m) for average a_o/w of 0.3, 0.5, and 0.7 respectively. For load-controlled beams, the average

values of U were 1.24 lb-in (0.140 N-m), 0.574 lb-in (0.0649 N-m), and 0.246 lb-in. (0.0278 N-m), for average a_o/w of 0.3, 0.5, and 0.7 respectively.

The fracture energy per unit area was also calculated using the Modified RILEM Method for all sixteen beams. These values are listed in Table 4.2. As in Table 4.1, the "S" and "L" denote the loading mode.

Average values for $\overline{G_F}$ for strain-controlled beams were 0.202 lb-in./in.^{2} (35.3 N-m/m^2), 0.108 lb-in./in.^{2} (19.0 N-m/m^2), and 0.0625 lb-in./in.^{2} (11.0 N-m/m^2) for average a_o/w of 0.3, 0.5, and 0.7 respectively. Average values for $\overline{G_F}$ for load-controlled beams were 0.155 lb-in./in^2 (27.1 N-m/m^2), 0.104 lb-in./in.^{2} (18.2 N-m/m^2), and 0.0745 lb-in./in/^{2} (13.0 N-m/m^2) for average values of a_o/w ratio of 0.3, 0.5, and 0.7 respectively. Figure 4.3 shows plots of $\overline{G_F}$ versus average a_o/w using values from the Modified RILEM Method.

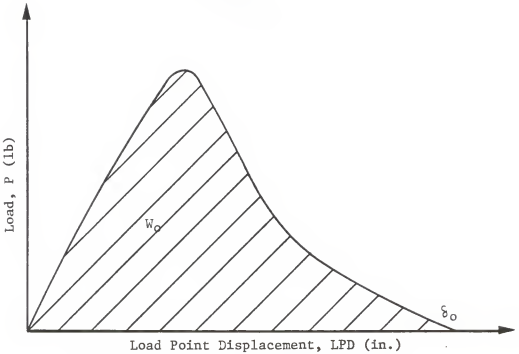

Figure 4.1 P vs LPD, RILEM Method, 3L.3

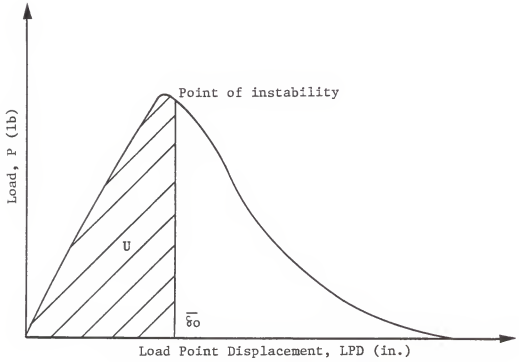

Figure 4.2 P vs LPD, Modified RILEM Method , 3L.3

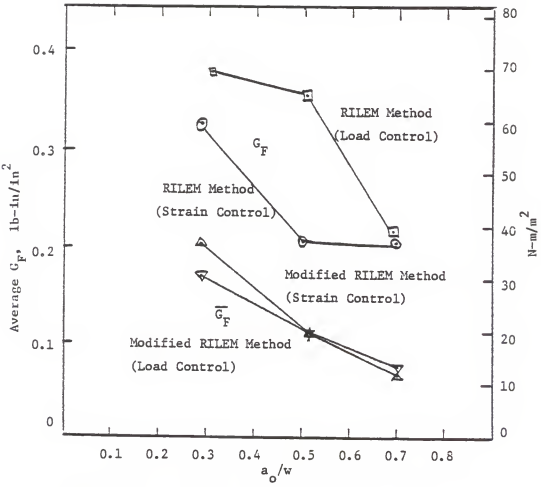

Figure 4.3 Average G_F Versus a_o/w, RILEM Method and Modified RILEM Method

Table 4.1 Notched Beams, Tested July 1985, RILEM Method, W = 4.00 in (102 mm), E_c = 5.02 x 10^6 psi (34.6 GPa)

Beam No.	Nominal a_o/w	a_o in mm	P_m lb N	Time to peak sec	δ_o in x 10^{-3} mm	W_o lb-in N-m	G_F lb-in/in^2 N-m/m^2
1S.3	0.3	1.16	710	34	10.20	2.27	0.285
		29.5	3160		0.259	0.257	50.0
2S.3		1.12	740	225	8.90	2.43	0.297
		28.4	3300		0.226	0.276	52.1
3S.3		1.12	690	150	10.10	3.11	0.378
		28.4	3070		0.257	0.352	66.3
1L.3	0.3	1.32	670	167	13.9	3.10	0.413
		33.5	2980		0.353	0.350	72.4
2L.3		1.20	710	191	13.9	2.30	0.300
		30.5	3160		0.353	0.260	52.5
3L.3		1.16	690	183	14.3	3.33	0.417
		29.5	3070		0.363	0.376	73.1
1S.5	0.5	2.00	360	60	9.30	1.10	0.208
		50.8	1600		0.236	0.124	36.4
2S.5		2.00	360	37	7.70	0.960	0.180
		50.8	1600		0.196	0.108	31.5
3S.5		2.04	360	51	8.50	1.20	0.227
		51.8	1600		0.216	0.136	39.7
1L.5	0.5	2.04	335	60	14.2	1.68	0.323
		51.8	1490		0.361	0.189	56.7
2L.5		2.00	410	72	15.1	2.25	0.414
		50.8	1820		0.384	0.254	72.6
3L.5		2.04	400	71	12.9	1.66	0.317
		51.8	1780		0.328	0.187	55.5
1S.7	0.7	2.80	130	54	8.60	0.547	0.189
		71.1	579		0.218	0.0618	33.1
3S.7		2.76	170	61	8.10	0.62	0.200
		70.1	757		0.206	0.0701	35.2
2L.7	0.7	2.68	160	84	8.20	0.621	0.189
		68.1	712		0.208	0.0701	33.1
3L.7		2.80	150	50	11.1	0.700	0.243
		71.1	668		0.282	0.0791	42.5

Notes 1. W/C = 0.50, C:S:A = 0.41 : 0.69 : 1, Max. Agg = 0.75 in (19 mm)

2. S = 15 in (381 mm), L = 16 in (406 mm), mg = 15.6 lb (7.08 Kg), f'_c = 6170 psi (42.5MPa)

Table 4.2 Notched Beams, Tested July 1985, Modified RILEM Method, W = 4.00in (102mm), E_c = 5.02 x 10^6 psi (34.6 GPa)

Beam No.	Nominal a_o/w	a_o in mm	P_m lb to peak N	Time sec	$\overline{\varepsilon_o}$ in x 10^{-3} mm	U lb-in N-m	$\overline{G_F}$ lb-in/in^2 N-m/m^2
1S.3	0.3	1.16	710	34	4.82	1.78	0.218
		29.5	3160		0.122	0.200	38.1
2S.3		1.12	740	225	3.67	1.46	0.176
		28.4	3300		0.0932	0.166	30.8
3S.3		1.12	690	150	5.00	1.75	0.212
		28.4	3070		0.127	0.197	37.1
1L.3	0.3	1.32	670	167	2.77	1.20	0.155
		33.5	2980		0.0704	0.136	27.1
2L.3		1.20	710	191	3.38	1.06	0.133
		30.5	3160		0.0859	0.119	23.2
3L.3		1.16	690	183	2.65	1.47	0.177
		29.5	3070		0.0673	0.166	31.1
1S.5	0.5	2.00	360	60	4.33	0.650	0.120
		50.8	1600		0.110	0.0735	21.0
2S.5		2.00	360	37	2.10	0.490	0.087
		50.8	1600		0.0533	0.0553	15.3
3S.5		2.04	360	51	3.31	0.640	0.118
		51.8	1600		0.0841	0.0723	20.6
1L.5	0.5	2.04	335	60	2.46	0.443	0.082
		51.8	1490		0.0625	0.0502	14.3
2L.5		2.00	410	72	3.19	0.752	0.134
		50.8	1820		0.0810	0.0849	23.4
3L.5		2.04	400	71	2.55	0.527	0.096
		51.8	1780		0.0648	0.0595	16.9
1S.7	0.7	2.80	130	54	2.67	0.179	0.061
		71.1	579		0.0678	0.0203	10.7
3S.7		2.76	170	61	2.48	0.200	0.064
		70.1	757		0.0630	0.0226	11.2
2L.7	0.7	2.68	160	84	2.10	0.272	0.077
		68.1	712		0.0533	0.0306	13.5
3L.7		2.80	150	50	2.41	0.220	0.0720
		71.1	668		0.0612	0.0249	12.5

Note: 1. For dimensions and material properties see Table 4.1.

Table 4.3 Summary of Average Values of Fracture Energy Parameters

Avg. a_o/w	Type of control	Avg. W_o lb-in N-m	Avg. U lb-in N-m	Avg. δ_o in x 10^{-3} m	Avg. $\overline{\delta_o}$ in x 10^{-3} m	Avg. G_F lb-in/in^2 N-m/m^2	Avg. $\overline{G_F}$ lb-in/in^2 N-m/m^2
0.283	Strain	2.60	1.66	9.73	4.50	0.320	0.202
		0.295	0.188	0.247	0.114	56.1	35.3
0.307	Load	2.91	1.24	14.03	2.93	0.377	0.155
		0.329	0.140	0.366	0.0745	66.0	27.1
0.503	Strain	1.09	0.593	8.50	3.25	0.205	0.108
		0.123	0.0670	0.216	0.0825	35.9	19.0
0.507	Load	1.86	0.574	14.1	2.73	0.351	0.104
		0.210	0.0649	0.358	0.0694	61.6	18.2
0.695	Strain	0.584	0.190	8.35	2.58	0.195	0.0625
		0.0660	0.0215	0.212	0.0654	34.2	11.0
0.685	Load	0.661	0.246	9.65	2.26	0.216	0.0745
		0.0746	0.0278	0.245	0.0573	37.8	13.0

CHAPTER 5

SUMMARY AND CONCLUSIONS

The experimental results are interpreted and summarized as follows:

1. The shapes of traces of load versus LPD for both load-controlled and strain-controlled beams were very similar.
2. The time to peak load in this research ranged from 34 to 225 seconds (see Appendix II). Values of G_F obtained in this range showed fairly consistent results. However, if the ASTM Standard load rate for flexure is used instead, time to peak load should have a range of about 234 to 432 seconds based on modulus of rupture of 683 psi (4.71 MPa) and 901 psi (6.21 MPa). Factors that will affect this time range are initial notch length, size, and peak load of the beam. Therefore, a systematic computation technique for time to peak load is desired for testing beams in three-point bending for fracture energy in order to obtain consistent and useful results.
3. Using the RILEM Method, the energy consumed by the beams using load control and the related values of G_F were consistently greater than for the beams using strain control.
4. Using the Modified RILEM Method, the energy consumed by the beams and the related values of G_F were indifferent to the mode of control. Thus, this method is more consistent in determining G_F. This method also provided greater flexibility in determining G_F since both strain control or load control can be used during testing.
5. Values of G_F obtained in the experimental work vary with a_o/w as has

been noted before (34) since the beams were not precracked and/or crack growth (extension) was not considered. The values of G_F range from 0.202 lb-in./in.^{2} (35.3 N-m/m^2) to 0.0625 lb-in./in.^{2} (11.0 N-m/m^2). If the J-integral method is used (11,32,34), the value of $G_F = J_{IC}$ is 0.219 lb-in./in.^{2} (38.4 N-m/m^2). See Fig. 5.1.

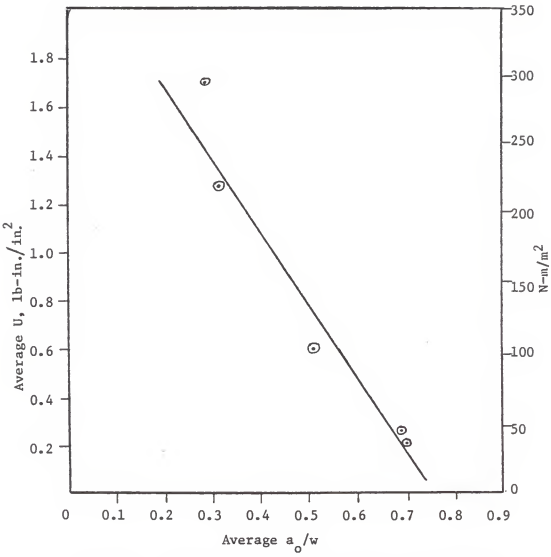

Figure 5.1 Determination of J_{IC} Using Average Values of Notch Length and Energy to Point of Instability

APPENDIX I

REFERENCES

1) ASTM C39-81, "Compressive Strength of Cylindrical Concrete Specimens," American Society for Testing and Materials, Philadelphia, USA, 1983.

2) ASTM C78-75, "Flexural Strength of Concrete," American Society for Testing and Materials, Philadelphia, USA, 1983.

3) ASTM C192-76, "Making and Curing Concrete Test Specimens in the Laboratory," American Society for Testing and Materials, Philadelphia, USA, 1983.

4) ASTM C496-71,"Splitting Tensile Strength of Cylindrical Concrete Specimens," American Society for Testing and Materials, Philadelphia, USA, 1983.

5) Bazant, Z. P., "Fracture Energy of Concrete from Maximum Loads of Specimens of Various Sizes," Proposal for RILEM Recommendation, Northwestern Univ., Evanston, IL, 1985.

6) BS 1881: Part 1, 4, "Methods of Concrete Testing," British Standard Institution, London, 1970, pp 16, 26.

7) Brown, J. H., and Pomeroy, C. D., "Fracture Toughness of Cement Paste and Mortars," Cement and Concrete Research, 3, 1973, pp 475-480.

8) Dilger, W. H., Kosch, R., and Kowalczyk, R., "Ductility of Plain and Confined Concrete Under Different Strain Rates," ACI Journal, Proceedings, V. 81, No. 11, Jan-Feb, 1984, pp. 73-81.

9) Galloway, J. W., and Raithby, K. D., "Effect of Rate of Loading on Fatigue Strength and Fatigue Performance," Transport and Road Research Laboratory Report LR547, pp. 10, Crowthrne, Berks., 1973.

10) Go, C. C. and Swartz, S. E, "Fracture Toughness Techniques to Predict Crack Growth and Tensile Failure in Concrete," Report 154, Engineering Experiment Station," Kansas State Univ., Manhattan, KS, July, 1983.

11) Go, C. C., and Swartz, S. E., " Energy Method for Fracture Toughness Determination in Concrete," Proceedings, Vth International Congress on Experimental Techniques, Montreal, June 10-14, 1984.

12) Higgins, D. D., and Bailey, J. E., "Fracture Measurements on Cement Paste," Journal of Material Science, 11, 1976, pp. 1995-2003.

13) Hillerborg, Arne, "Concrete Energy Tests Performed by Laboratories According to RILEM Recommendation," Report TVBM-3015, Lund Institute of Technology, Division of Buliding Materials, Lund, Sweden, 1983.

14) Hillerborg, Arne, "Additional Concrete Fracture Energy Tests Performed by 6 Laboratories According to a Draft RILEM Recommendation," Report TVBM-3017, Lund Institute of Technology, Division of Building Materials, Lund, Sweden, 1984.

15) Hillerborg, Arne, "Influence of Beam Size on Concrete Fracture Energy Determined According to a Draft RILEM Recommendation," Report TVBM-3021, Lund Institute of Technology, Division of Building Materials, Lund, Sweden, 1985.

16) Hilsdorf, H. K., and Brameshuber, W., "Size Effects in the Experimental Determination of Fracture Mechanics Parameters," Preprints of the Proceedings, NATO Advanced Research Workshop on Application of Fracture Mechanics to Cementitious Composites, Northwestern Univ., Evanston, IL, 1984, pp. 255-288.

17) Komlos, K., "Factors Affecting the Stress-Strain Relation of Concrete in Uniaxial Tension," ACI Journal, Proceedings, V. 66, No. 11, Feb. 1969, pp. 111-114.

18) Lin, T. C., and McDonald, J. E., "Prediction of Tensile Strain Capacity of Mass Concrete," ACI Journal, Proceedings, V. 75, No. 20, May, 1978, pp. 192-197.

19) McHenry, D., and Shideler, J. J., "Review of Data on Effect of Speed in Mechanical Testing of Concrete," ASTM Special Technical Publications, No. 185, pp. 72-82, 1956.

20) McNeely, D. J., and Lash, S. D., "Tensile Strength of Concrete," ACI Journal, Proceedings, V. 60, June 1963, pp. 751-761.

21) Newman, K., "The structure and properties of concrete- An Introductory Review," Proceedings, International Conference on Structure and Solid Mechanics, Southampton, 1969.

22) Petersson, P., "Crack Growth and Development of Fracture Zones in Plain Concrete and Similar Materials," Report TVBM-1006, Lund Institute of Technology, Division of Building Materials, Lund, Sweden, 1981.

23) Price, W. H., "Factors Influencing Concrete Strength," ACI Journal, Proceedings V. 47, No. 31, Feb. 1951, pp. 417-432.

24) RILEM Technical Committee 50-FMC, "Determination of the Fracture Energy of Mortar and Concrete by Means of Three-Point Bend Tests on Notched Beams," Proposed RILEM Recommendation, Jan. 1982, Revised June 1982, Lund Institute of Technology, Division of Building, Lund, Sweden.

25) Rood, S., "Fracture Toughness Testing of Small Concrete Beams," Master's Thesis, Department of Civil Engineering, Kansas State University, Manhattan, KS, 1984.

26) Rüsch, H., "Physikalische Fragen der Betonprufung," Zement-Kalk-Gips, 12, (1), 1959, 1-9.

27) Swamy, R. N., "Linear Elastic Fracture Mechanics Parameters of Concrete," Fracture Mechanics of Concrete, F. H. Whittman, ed., Elsevier Science Publishers B.V., Amsterdam, Netherlands, 1983, pp. 411-461.

28) Swartz, S. E., Hu, K. K., and Jones, G. L., "Compliance Monitoring of Crack Growth in Plain Concrete," Journal, Engineering Mechanics Division, ASCE, V. 104, No. EM4, Aug. 1978.

29) Swartz, S .E., Hu, K. K., Huang, C. J., and Fartash, M, "Stress Intensity Factors for Plain Concrete in Bending - Prenotched Beams Versus Precracked Beams," Experimental Mechanics, Vol. 22, No. 11, Nov. 1982.

30) Swartz, S. E., Huang, C. J., and Hu, K. K., "Crack Growth and Fatigue in Plain Concrete - Static Versus Fatigue Loading," Fatigue of Concrete Structures, Shah, S. P., ed., ACI Special Publication SP-75, ACI, Detroit, Michigan, MI, 1982.

31) Swartz, S. E., "Fracture Toughness Testing of Concrete at Kansas State University: Is LEFM Accetable?," Preprints, Vol. 11, Int. Conf. on Fracture Mechanics of Concrete, Lausanne, 1-3 Oct, 1985.

32) Swartz, S. E., and Go, C. C., "Validity of Compliance Calibration to Cracked Beams in Bending," Experimental Mechanics, Vol. 24, No. 2, June 1984.

33) Swartz, S. E., and Rood, S., "Fracture Toughness Testing of Concrete Beams in Three-Point Bending: Phase I, Small Beams," Proceedings, 1985 Spring Conference on Experimental Mechanics, Las Vegas, NV, June 9-14, 1985.

34) Swartz, S. E., and Yap, S. T., "Evaluation of Recently Proposed Recommendations for the Determination of Fracture Parameters for Concrete in Bendings," Proceedings, VIIIth International Conference on Experimental Stress Analysis," Amsterdam, May 12-16, 1986.

35) Wright, P. J. F., "The Effect of Method of Test on the Flexural Strength of Concrete, Magazine of Concrete Research, 4, No. 11, pp. 67-76.

36) Ziegeldorf, S., "Linear Elastic Fracture Mechanics Parameters for Concrete," Fracture Mechanics of Concrete, F. H. Whittman, ed. Elsevier Science Publishers B. V., Amsterdam, Netherlands, 1983, pp. 463-480.

APPENDIX II

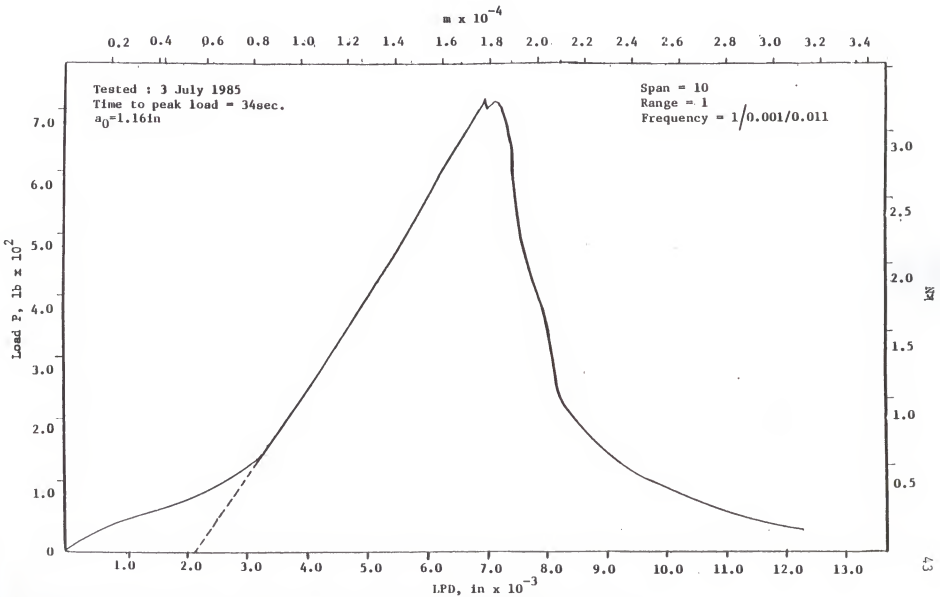

Fig. A1 P vs LPD, 4 in Deep Beam (1S.3), Strain Control, Tested July 1985

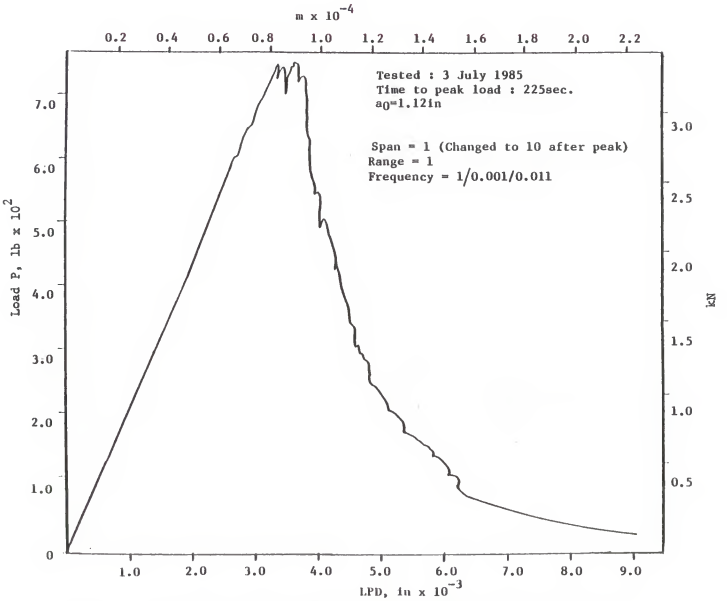

Fig. A2 P vs LPD, 4 in Deep Beam (2S.3), Strain Control, Tested July 1985

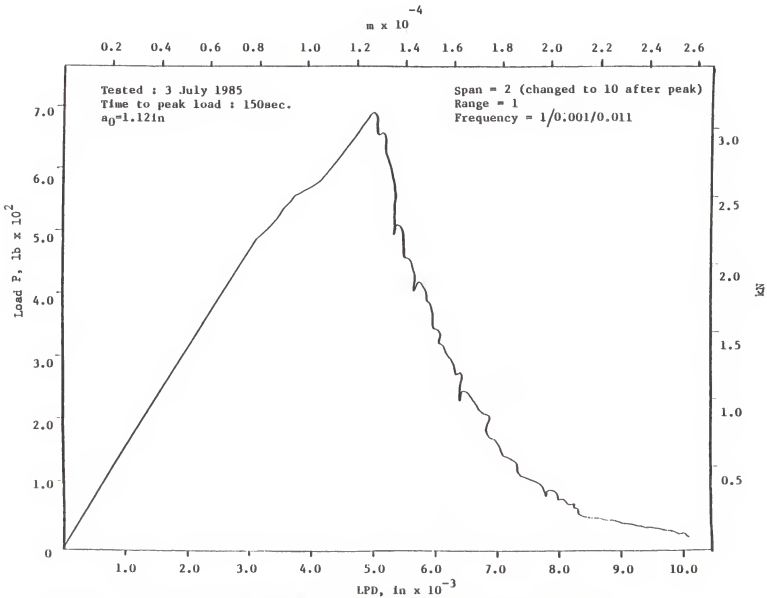

Fig. A3 P vs LPD, 4 in Deep Beam (3S.3), Strain Control, Tested July 1985

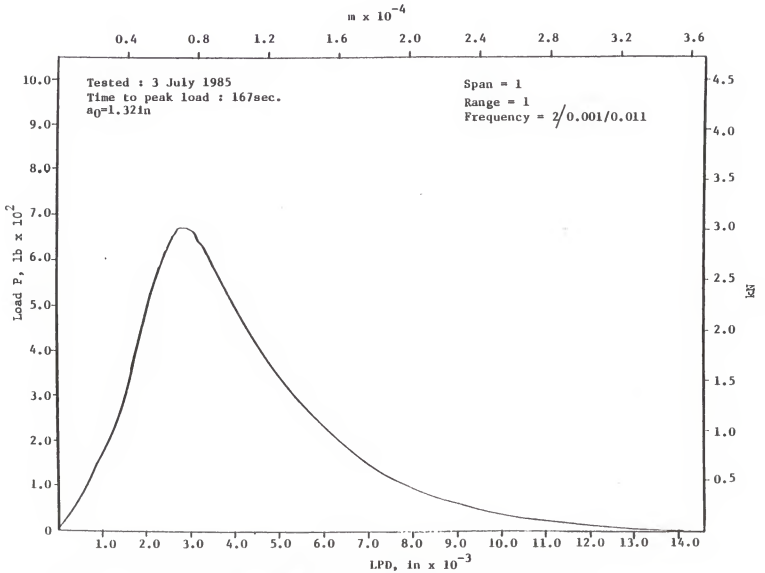

Fig. A4 P vs LPD, 4 in Deep Beam (IL.3), Load Control, Tested July 1985

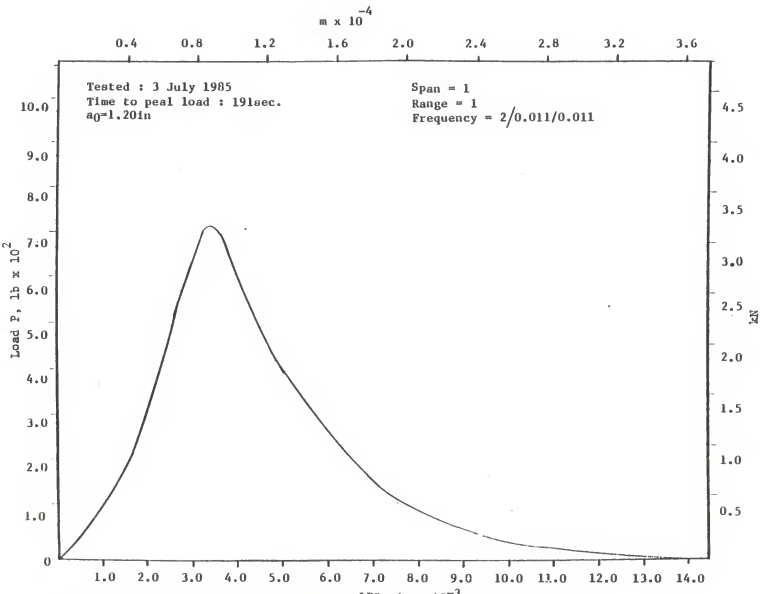

Fig.A5 P vs LPD, 4 in Deep Baem (2L.3), Load Control, Tested July 1985

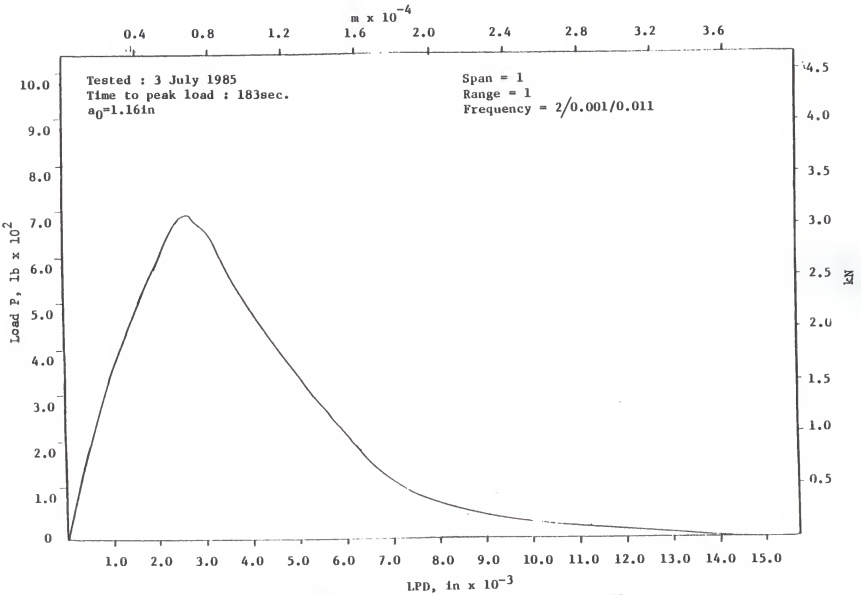

Fig. A6 p vs LPD, 4 in Deep Beam (3L.3), Load Control, Tested July 1985

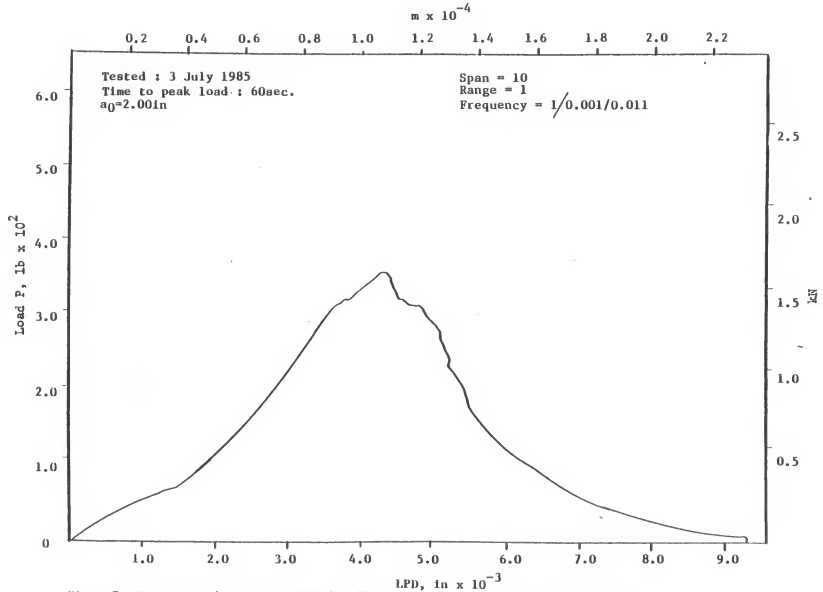

Fig. A7 P vs LPD, 4 in Deep Beam (1S.5), strain Control, Tested July 1985

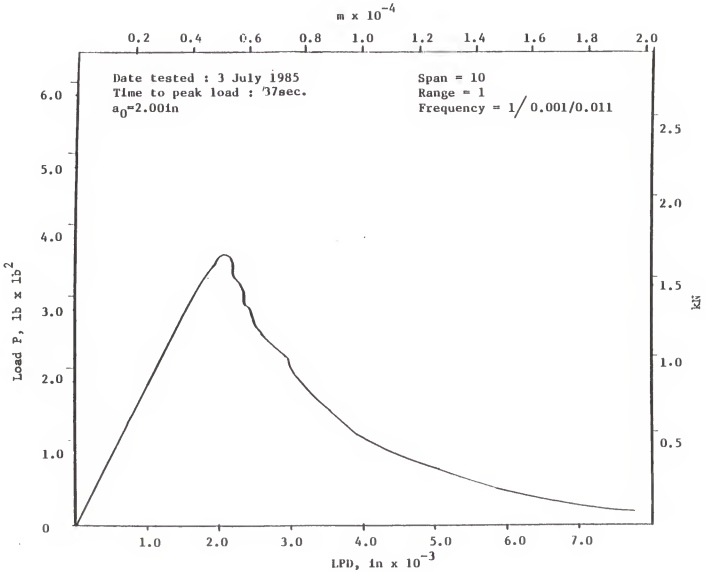

Fig. A8 P vs LPD, 4 in Deep Beam (2S.5), Strain Control, Tested July 1985

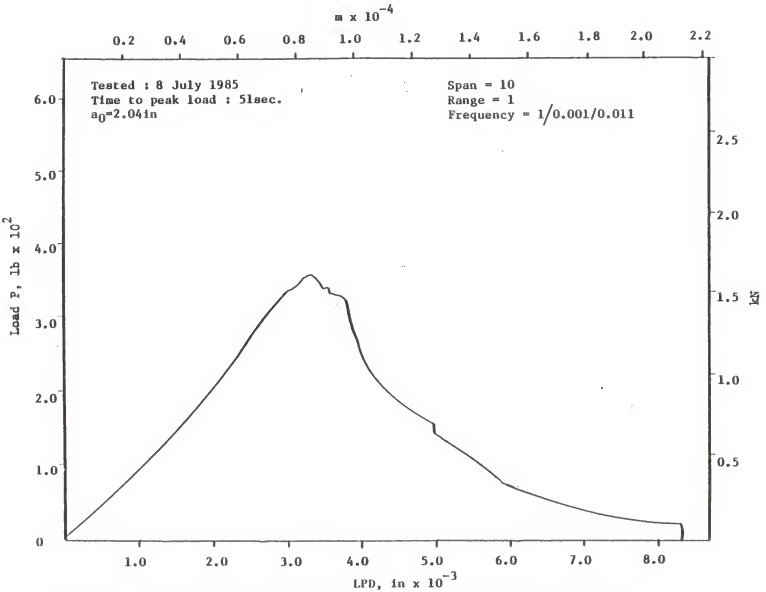

Fig. A9 P vs LPD, 4 in Deep Beam (3S.5), Strain Control, Tested July 1985

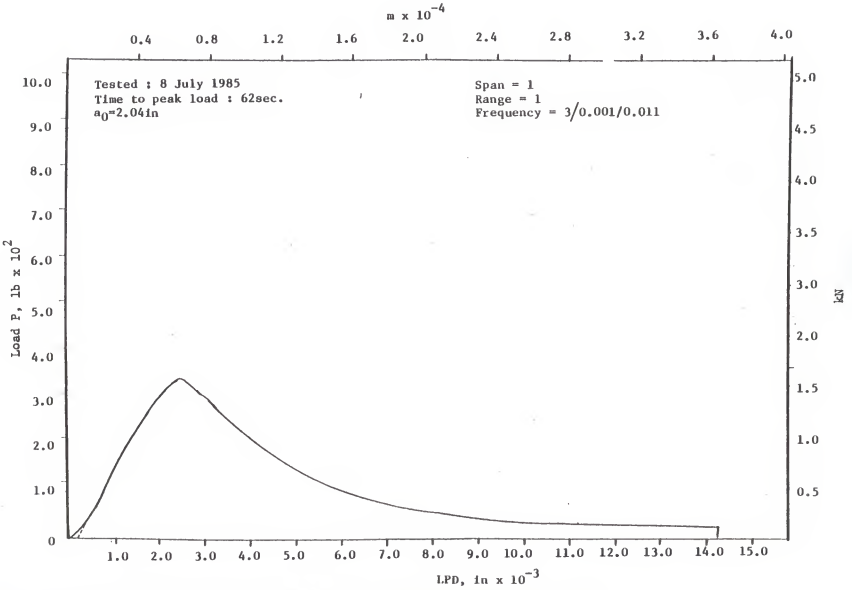

Fig. A10 P vs LPD, 4 in deep Beam (1L.5), Load Control, Tested July 1985

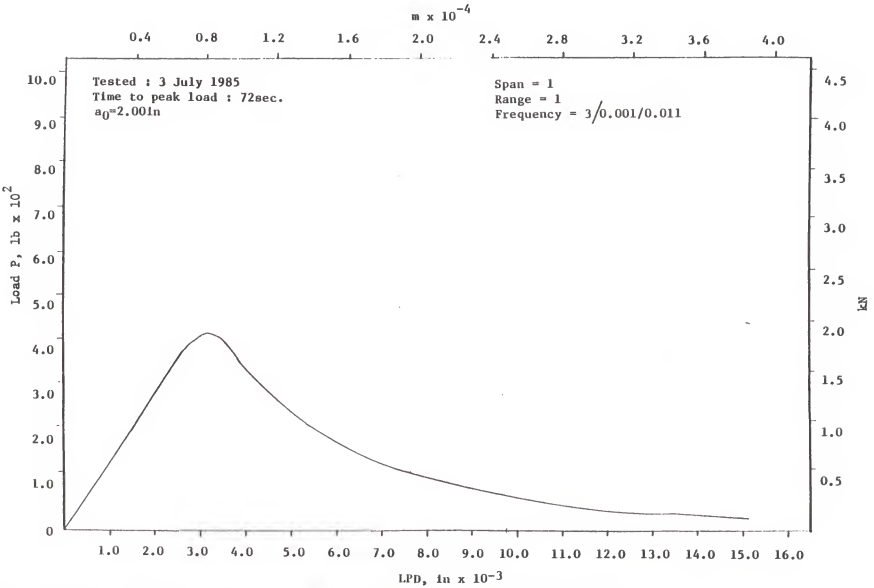

Fig. A11 P vs LPD, 4 in Deep Beam (2L.5), Load Control, Tested July 1985

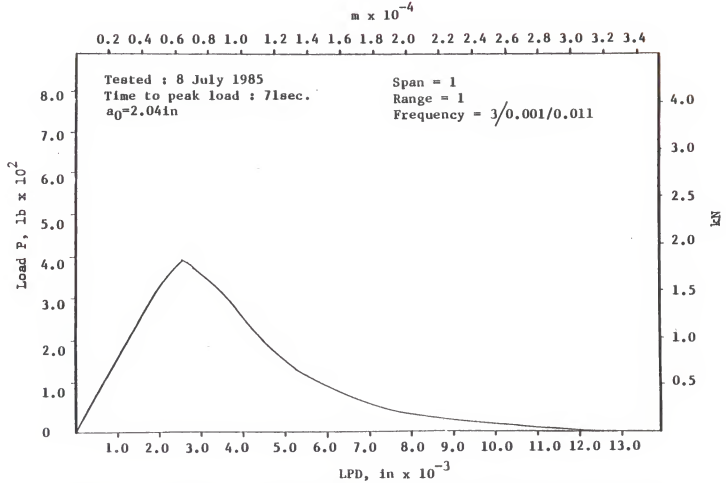

Fig. A12 P vs LPD, 4 in Deep Beam (3L.5), Load Control, Tested July 1985

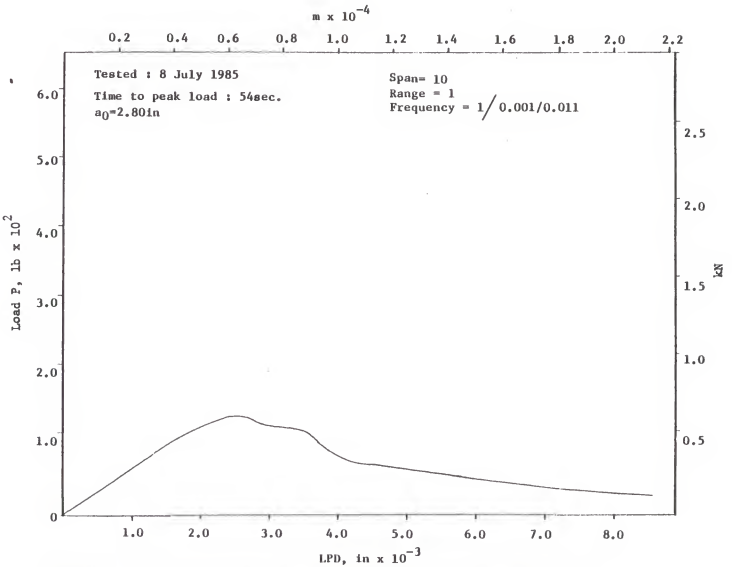

Fig. A13 P vs LPD, 4 in Deep Beam (1S.7), Srain Control, Tested July 1985

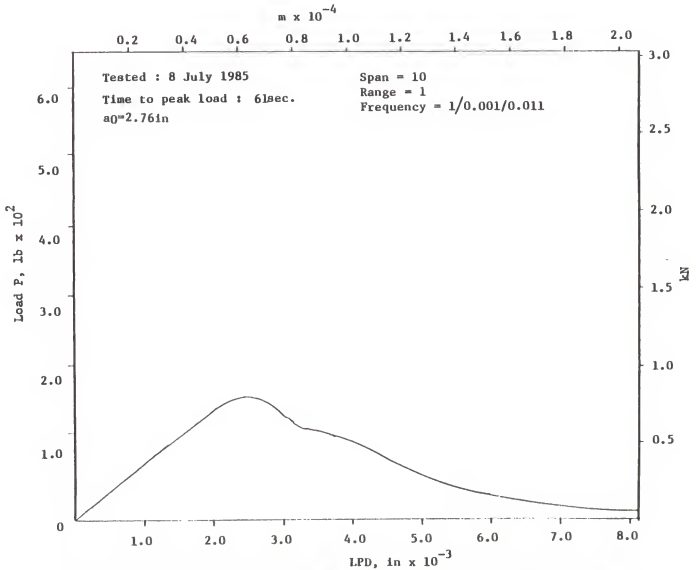

Fig. A14 P vs LPD, 4 in Deep Beam (3S.7), strain Control, Tested July 1985

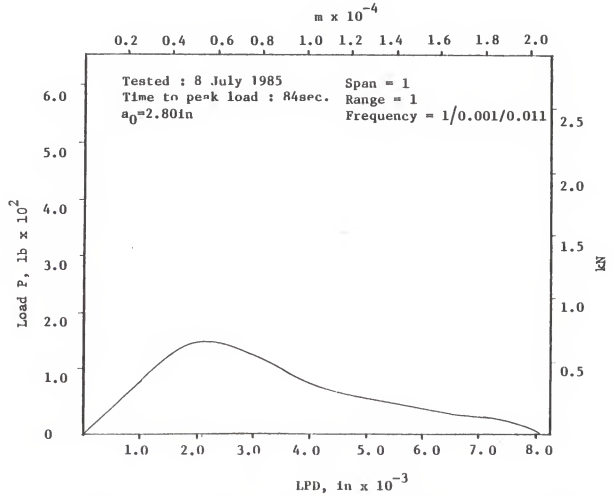

Fig. A15 P vs LPD, 4 in Deep Beam (2L.7), Load Control, Tested July 1985

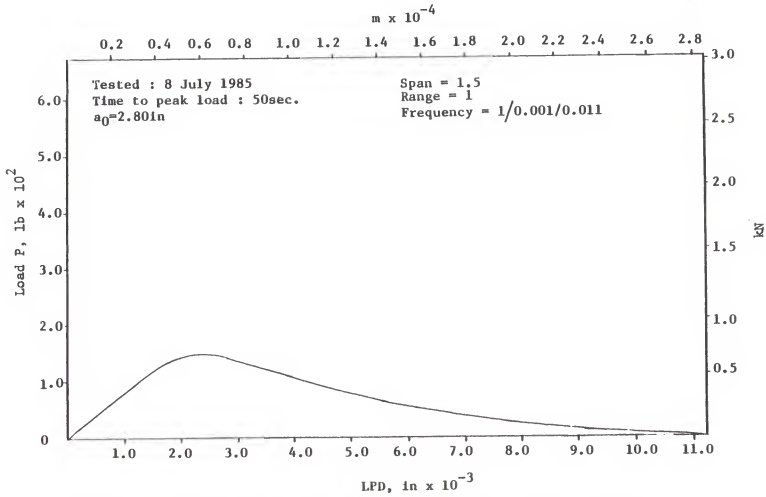

Fig. A16 P vs LPD, 4 in Deep Beam (3L.7), Load Control, Tested July 1985

TIME EFFECTS IN THE STATIC TESTING OF CONCRETE TO DETERMINE FRACTURE ENERGY

by

Hoi Choong Siew

B.S., Kansas State University, 1984

AN ABSTRACT OF A MASTER'S THESIS

submitted in partial fulfillment of the

requirements for the degree of

MASTER OF SCIENCE

Department of Civil Engineering

KANSAS STATE UNIVERSITY

Manhattan, Kansas

1986

ABSTRACT

An experimental program was carried out to study the effects of time in the static testing of concrete to determine fracture energy (G_F). Although it is widely known that the time does affect testing results of concrete in compression, flexure, and tension, little is known how it affects G_F of concrete.

Beams of one size of 3 in. wide, 4 in. deep, and 15 in. span with a_o/w of 0.3, 0.5, and 0.7 were used in the experimental program. These beams were loaded to failure with load control and strain control with time to peak ranging from 34 to 225 seconds. Values of G_F obtained in the periods of time used in the experiment were relatively consistent. To obtain consistent and relevant results, a systematic computation technique for time to peak load is desired where it will depend on the initial notch length, size, and peak load of the beam. G_F was calculated in two manners, the RILEM Method and the Modified RILEM Method. Comparisons were then made of G_F values obtained using the two mentioned methods and different modes of controls. Using the RILEM Method, G_F showed consistently higher results when load control was used then when compared to strain control. However, when the Modified RILEM Method was used, the mode of control did not affect the results of G_F.